



**Thank you for downloading this document from the RMIT Research Repository.**

The RMIT Research Repository is an open access database showcasing the research outputs of RMIT University researchers.

RMIT Research Repository: <http://researchbank.rmit.edu.au/>

**Citation:**

**See this record in the RMIT Research Repository at:**

**Version:**

**Copyright Statement:**

©

**Link to Published Version:**

**PLEASE DO NOT REMOVE THIS PAGE**



6th Asia Pacific Workshop on Structural Health Monitoring, 6th APWSHM

## Using Carbon Nanofibre Sensors for In-situ Detection and Monitoring of Disbonds in Bonded Composite Joints

Raj B. Ladani<sup>a</sup>, Shuying Wu<sup>a</sup>, Jin Zhang<sup>b</sup>, Kamran Ghorbani<sup>a</sup>, Anthony J. Kinloch<sup>c</sup>, and Adrian P. Mouritz<sup>a</sup> and Chun H. Wang<sup>d\*</sup>

<sup>a</sup>School of Engineering, RMIT University, GPO Box 2476, Melbourne-Vic3001, Australia

<sup>b</sup>Institute for Frontier Materials, Deakin University, Geelong Warun Ponds Campus, Geelong-Vic3220, Australia

<sup>c</sup>Department of Mechanical Engineering, Imperial College London, South Kensington Campus, London-SW72AZ, United Kingdom

<sup>d</sup>School of Mechanical and Manufacturing Engineering, University of New South Wales, Sydney-NSW3220, Australia

### Abstract

This paper focuses on the ability of carbon nanofibre (CNF) networks to in situ monitor fatigue induced disbond damage in adhesive bonded composite joints. The inclusion of CNFs in the epoxy adhesive increases its conductivity by five orders of magnitude. The improved electrical conductivity is utilized to evaluate the ability of the CNF network to monitor and detect the fatigue induced disbond damage by measuring the *in-situ* resistance changes using a four probe setup. The changes in total resistance was a function of the bulk electrical resistivity of the adhesive and the bond dimensions, which were related to the disbond length to model and determine the size of the disbond. The simple resistivity model was in good agreement with the resistance measured during fatigue testing. Good agreement was found between the optical disbond observations and the disbond length calculated using the proposed model. Finite element simulations were performed to ascertain the range of applicability of the proposed model. The simplicity of the disbond detection technique via direct current potential drop technique enables real time monitoring of crack growth in the composite structure.

© 2016 The Authors. Published by Elsevier Ltd. This is an open access article under the CC BY-NC-ND license (<http://creativecommons.org/licenses/by-nc-nd/4.0/>).

Peer-review under responsibility of the organizing committee of the 6th APWSHM

**Keywords:** Carbon nanofibre, adhesive, nanocomposite, damage detection, structural health monitoring.

\* Corresponding author. Tel.: +61-2-93854006.  
E-mail address: [chun.h.wang@unsw.edu.au](mailto:chun.h.wang@unsw.edu.au)

## 1. Introduction

One of the key challenge for using composites as load-bearing safety-critical structures is the need for detecting and quantifying disbonds to ensure continuing structural integrity. While adhesively bonded joints provide many advantages such as low cost, high strength to weight ratio, low stress concentration, fewer processing requirements and good environmental resistance [1], the dielectric characteristic of existing structural adhesives means that most conductivity-based techniques, such as eddy current, potential drop, and electrical impedance, are not suitable for detection of bondline flaw or damage [2]. Recent studies have shown that conductive carbon nanofillers such as carbon nanotubes (CNTs) [3, 4] or carbon nanofibres (CNFs) [5-7] can form conductive networks in polymeric materials at extremely low weight fractions while simultaneously improving the fracture toughness. These conductive networks offer a new route for *in-situ* health monitoring of adhesively bonded structures.

### Nomenclature

$\sigma_1$	conductivity of the composite substrate
$\sigma_2$	conductivity of the adhesive
$\Delta a$	disbond length
$t_a$	adhesive thickness
$t_c$	composite substrate thickness
$b$	width of the joint
$l_b$	adhesive bondline length
$R$	resistance
$R_o$	initial resistance corresponding to no disband
$\Delta R$	change in resistance due to disbond

Recently, Lim et al. [8] reported the use of CNT networks to monitor the initiation of damage in epoxy bonded lap joints under quasi-static and dynamic tensile loading. Mactabi et al. [9] studied the electromechanical response of CNT networks incorporated in bonded lap joints under tensile fatigue loading. While a short communication by Zhang et al.[10] is the only study reported on utilizing CNT networks in epoxy polymer to monitor and predict the underlying crack growth damage during mode I fatigue testing. They successfully demonstrated that changes in resistance induced by mode I fatigue crack growth in bulk epoxy samples could be used to determine the size of the underlying damage. However, the potential application of this technique to monitor and detect fatigue crack growth in bonded composite joints has not been studied to date.

Considering that CNFs may be an excellent alternative to CNTs due to their wide availability and lower cost [11], the present study focuses on the use of CNFs to improve the electrical conductivity of an epoxy nanocomposite adhesive to enable the monitoring and detection of fatigue crack growth in bonded joints. The electrical response of the nanocomposite adhesive is measured *in-situ* during mode I fatigue crack growth using a DC potential drop technique. A simple resistivity model is developed to relate the size of the disbond with the electrical resistance. Finite element analyses are performed to verify the analytical model and to investigate the range of applicability of the simple resistivity model.

## 2. Materials and Experimental Details

The epoxy adhesive used for bonding composites was blend of five parts of bisphenol A '105' and one part of the hardener '206' (from West System). Commercially-available vapour-grown carbon nanofibres, Pyrograf® - III PR-24-HHT and supplied by Applied Sciences Inc., USA, were employed as the nanofiller. Carbon fibre composite substrates were manufactured using 12 plies of unidirectional T700 carbon fibre/epoxy prepreg (VTM 264 supplied by Applied Composites Group). The composite substrates, with dimensions of 100 mm x 100 mm x 2.5 mm, were cured and consolidated in an autoclave at 120 °C for 1 hr., in accordance with the manufacturer's recommended cure process. The substrate surfaces were abraded using 320 grit aluminium oxide abrasive paper, cleaned under running tap water for about 2 minutes, degreased with acetone, and finally cleaned with distilled water to remove any surface

impurities. A three-roll mill (Dermamill 100) was used to disperse the CNFs in the liquid epoxy resin. This CNF-modified epoxy resin mixture was then poured between the composite substrates. Spacers, 2 mm in thickness made of glass slides, were placed at both ends of the joint to control the thickness of the epoxy layer between the substrates. A Teflon-coated tape about 30 mm long and 11  $\mu\text{m}$  thick was placed at an approximately the centre of the adhesive layer at one end of the joint to act as a crack starter. The joints were allowed to cure under ambient conditions prior to cutting into 20 mm wide double-cantilever beam (DCB) adhesively-bonded specimens. Further details of the joint manufacturing and testing are given in our recent publications [4-7, 12, 13].

The *in-situ* resistance characterisation study was conducted on 20 mm x 100 mm DCB samples as shown in **Fig. 1**. These samples had an initial bondline length of 50 mm. The Teflon insert was removed prior to the *in-situ* resistance testing. Electrodes were bonded to the composite substrates using a conductive silver paste. Non-conductive loading grips were used for electrically isolating the samples from the load frame. The specimen were subjected to mode I cyclic fatigue loading at a constant load of about 60 N and a load ratio (minimum load to maximum load) of 0.5. The fatigue tests were conducted in accordance to the ASTM E647 standard on a 3 kN electromagnetic pulse driven Instron E3000 fatigue test rig. During fatigue tests electric resistance was measured by a four probe resistance measurement technique using Delloger80 dataker. The crack lengths were recorded using a travelling microscope.

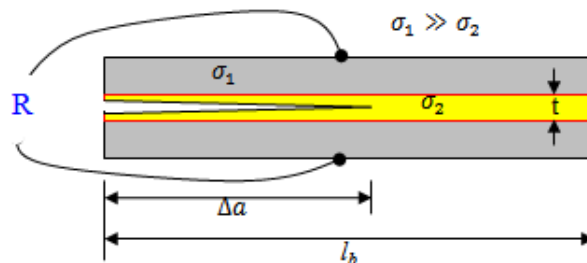


Fig. 1. Schematic of the double cantilever beam (DCB) composite joint used for mode I cyclic fatigue testing.

### 3. Results and Discussion

#### 3.1. *In-situ* resistance response during fatigue testing

The addition of CNFs to the adhesive led to a significant increase in its electrical conductivity. The addition of just 0.7 wt% CNF to the epoxy adhesive increases its conductivity by five orders of magnitude to  $10^{-4}$  S/m. This increase in conductivity due to the formation of percolating network of CNF enabled the use of electrical response to monitor disbond length. As shown in **Fig. 2a**, the resistance increased monotonically with increasing number of cycles. **Fig 2b** shows the effect of displacement on the transient resistance measurements recorded during cycling. The noise in the resistance signal emanating from the dataker was significantly low in comparison to the total resistance. While the larger undulations in the resistance signal were due to the loading and unloading of the DCB specimens, the resistances at the maximum and the minimum applied load increased with crack length. An irreversible increase in resistance after each cycle can be readily observed. This increase in resistance likely corresponds to the disbond of adhesive that reduces the conductive area of the adhesive bond. The disbond grew near the centre line of the adhesive layer, as shown in **Fig. 3**. The crack growth through the adhesive leads to the pull-out and rupture of the CNFs, which modifies the charge conduction pathways within the CNF-modified adhesive.

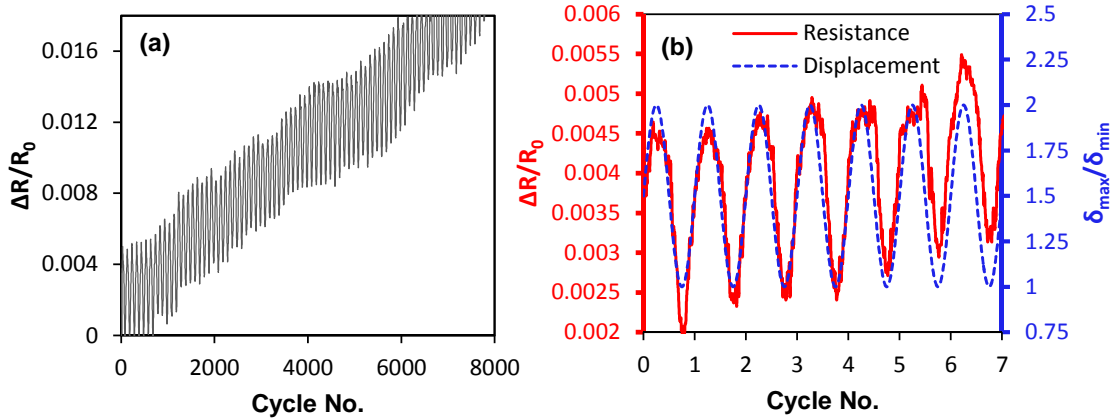


Fig. 2. *In-situ* resistance response during mode I cyclic fatigue testing at (a) 5 Hz and (b) 0.01 Hz fatigue cycling.

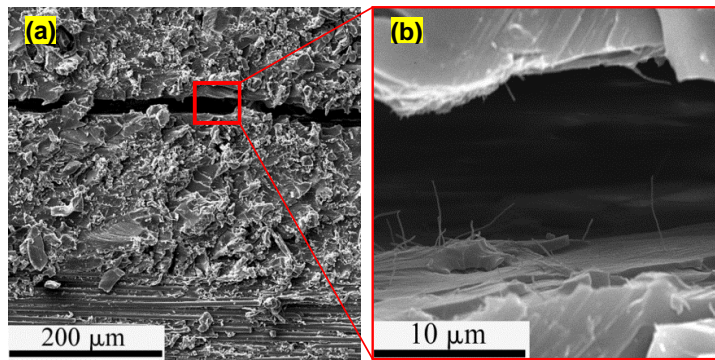


Fig. 3. SEM micrograph of the (a) fatigue test sample showing cohesive damage through the CNF modified adhesive leading to (b) the crack bridging and pull-out of CNFs from the adhesive.

The change in the total resistance at the maximum applied load is due to the shortening of the un-cracked ligament ahead of the crack tip. In the limit of composite adherends being significantly more conductive than the adhesive layer, the total resistance is a function of the electrical resistivity and geometrical dimensions (width and length) of the adhesive. A simple relationship between the total electrical resistance and the disbond length,  $\Delta a$ , can be developed by neglecting the resistance of the composite adherends,

$$R = \frac{t}{\sigma_2(l_b - \Delta a)b} \tag{1}$$

where  $\sigma_2$ ,  $l_b$ ,  $t$ ,  $b$ , and  $R$  denote the electric resistivity of the CNF-reinforced adhesive, the initial length, thickness and width of the adhesive, and the total resistance, respectively, as shown in **Fig. 1**. A comparison of the above relationship, i.e. Eq. (1), to the experimentally measured resistance as a function of disbond length is shown in **Fig.4a** and **Fig.4b**. The increase in resistance caused by the fatigue cracking is in good agreement with the change in resistance estimated by Eq. (1). Therefore, as shown in **Fig.4a** the increase in resistance measured *in-situ* can be used to detect the crack length. In **Fig.4b**, the disbond length calculated from Eq. (1) from the *in-situ* resistance measurements is in good agreement with the optical observation of the fatigue crack growth. Thus, the changes in

resistance could be effectively used to detect and monitor the growth of disbond in composite joints bonded with a reasonably conductive adhesive material.

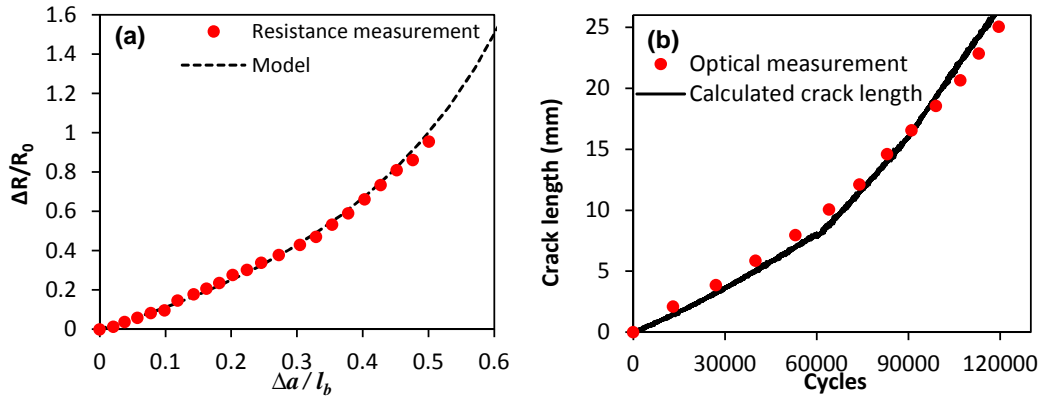


Fig. 4. (a) changes in resistance measured *in-situ* during fatigue testing and its comparison to the model Eq. (1); and (b) the disbond length calculated from Eq. (1) using the *in-situ* resistance measurements and its comparison to the optical observations of the disbond length .

### 3.2. Finite Element Analysis

The relationship given by Eq. (1) provides a limiting solution for composite adherends being infinitely conductive, i.e.  $\sigma_1 \gg \sigma_2$ . But its exact range of applicability for adherends of finite conductivity remains unknown. To ascertain the applicability of Eq. (3), finite element (FE) analysis was conducted to examine the effect of the ratios of  $\sigma_1/\sigma_2$  and  $\Delta a/l_b$  on the resistance response of the DCB joints. Finite element analysis was performed using the ANSYS® Maxwell3D software package. As shown in Fig. 5, a three-dimensional (3D) geometry representing the adhesive bonded composite joint was used for the simulations. The model consisted of the composite substrates, the adhesive layer and the solder contact materials. The electrical properties of the materials used for FE analysis are listed in Table 1. The bulk conductivity of the adhesive materials was varied from  $10^{-4}$  to 10 S/m to investigate its effects on the electrical resistance of the composite joint. The electrical simulation of the composite joint was performed with the direct current (DC) conduction solution. A DC excitation potential of 10 V was applied to the solder material (see Error! Reference source not found.b) to compute the current density through the thickness of the joint. The convergence of the solution was confirmed by using the in-built adaptive mesh refinement algorithm of the Maxwell3D software. The convergence criteria for the adaptive pass was set such that the error between successive iterations was less than or equal to 1%.

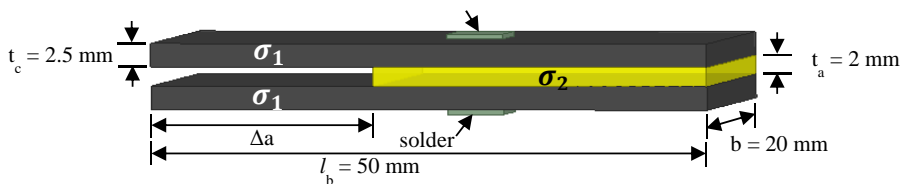


Fig. 5. 3D model of the composite joint used for the finite element simulations.

Table 1 Electrical conductivity and fatigue crack growth properties of the composite joints.

Material	Bulk Conductivity (S/m)	Relative Permeability
Composite substrate	1.0	1.0
Adhesive	$10^{-4}$ to 10.0	1.0
Solder	$7 \times 10^6$	1.0

**Fig. 6a** shows the effects of the conductivity ratio  $\sigma_1/\sigma_2$  on the electrical resistance obtained from FE simulations and its comparison to the resistance calculated from Eq. (1). It is clear that at high conductivity ratios, the resistance estimated by Eq. (1) is in good agreement with the numerical solutions. However, for conductivity ratios below 100, the resistance from the composite substrates becomes prominent and cannot be ignored. **Fig. 6b** shows the change in resistance due to a 50% reduction in adhesive bondline length as a function of the conductivity ratio. As can be seen in this figure, for conductivity ratio  $\sigma_1/\sigma_2$  greater than 1000, the resistance response obtained from FE simulations is very similar to the limiting solution of Eq. (1) and experimental result. In contrast, for conductivity ratio below 1000, the resistance caused by disbond is much less than that given by Eq. (1). The plots of the potential drop obtained from FE simulations given in **Fig. 7** suggest that as the adhesive conductivity increases the resistance change due to disbond growth decreases. Therefore, the limiting solution given by Eq. (1) is only valid for composite to adhesive conductivity ratios greater than 1000. Thus, the limiting solution should not be used to estimate the disbond length in composite laminates or structures bonded using highly conductive adhesives.

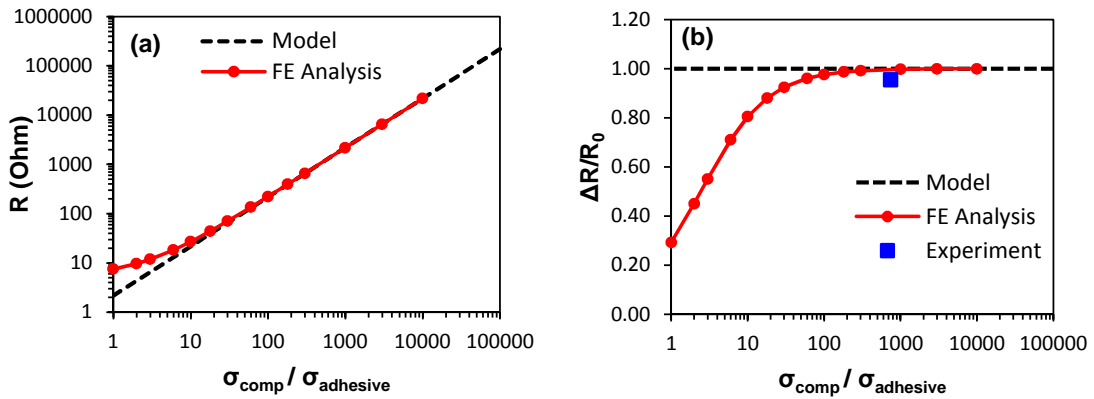


Fig. 6. (a) The resistance calculated from Eq. (1) and its comparison to the FE simulations; (b) The changes in resistance due to a 50% reduction in adhesive bondline length for various ratios of the composite to adhesive conductivities.

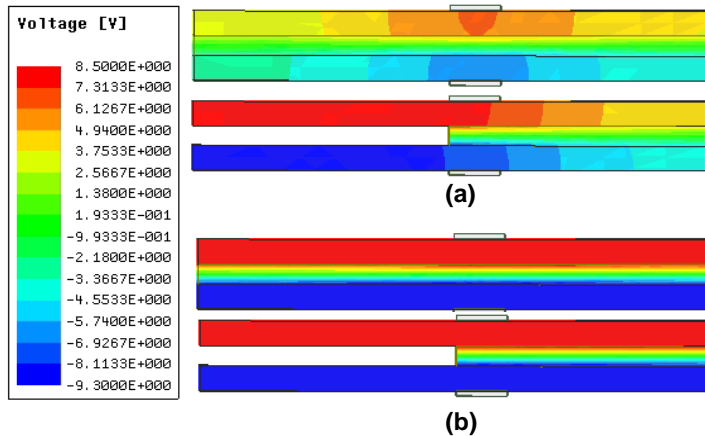


Fig. 7. Potential drop plots from FE simulations of the DCB joints corresponding to  $\Delta a/l_b$  equal to 0.5 and conductivity ratios equal to (a) 100, and (b) 1000.

#### 4. Conclusion

The electrical conductivity of epoxy adhesives can be improved by adding carbon nanofibers, which then allow disbond size to be determined by in situ monitoring changes in electrical resistance. In the case of adherends being highly conductive, such as carbon fibre laminates, a simple resistivity model has been developed to relate changes in resistance with the size of disbond. Both experimental measurements and computational modelling have confirmed that the validity of the simple model if the conductivity of the adhesive is 1000 times less than the composite substrates.

#### References

- [1] A.J. Kinloch, Adhesives in engineering, Proceedings of the Institution of Mechanical Engineers, Part G: Journal of Aerospace Engineering 211(5) (1997) 307-335.
- [2] R.D. Adams, P. Cawley, A Review of Defect Types and Nondestructive Testing Techniques for Composites and Bonded Joints, Ndt Int 21(4) (1988) 208-222.
- [3] S. Wu, R.B. Ladani, J. Zhang, E. Bafekrpour, K. Ghorbani, A.P. Mouritz, A.J. Kinloch, C.H. Wang, Aligning multilayer graphene flakes with an external electric field to improve multifunctional properties of epoxy nanocomposites, Carbon 94 (2015) 607-618.
- [4] S. Wu, J. Zhang, R.B. Ladani, K. Ghorbani, A.P. Mouritz, A.J. Kinloch, C.H. Wang, A novel route for tethering graphene with iron oxide and its magnetic field alignment in polymer nanocomposites, Polymer 97 (2016) 273-284.
- [5] R.B. Ladani, S. Wu, A.J. Kinloch, K. Ghorbani, J. Zhang, A.P. Mouritz, C.H. Wang, Improving the toughness and electrical conductivity of epoxy nanocomposites by using aligned carbon nanofibres, Composites Science and Technology 117 (2015) 146-158.
- [6] R.B. Ladani, S. Wu, A.J. Kinloch, K. Ghorbani, J. Zhang, A.P. Mouritz, C.H. Wang, Multifunctional properties of epoxy nanocomposites reinforced by aligned nanoscale carbon, Mater Design 94 (2016) 554-564.
- [7] S. Wu, R.B. Ladani, J. Zhang, A.J. Kinloch, Z. Zhao, J. Ma, X. Zhang, A.P. Mouritz, K. Ghorbani, C.H. Wang, Epoxy nanocomposites containing magnetite-carbon nanofibers aligned using a weak magnetic field, Polymer (United Kingdom) 68 (2015) 25-34.
- [8] A.S. Lim, Z.R. Melrose, E.T. Thostenson, T.W. Chou, Damage sensing of adhesively-bonded hybrid composite/steel joints using carbon nanotubes, Composites Science and Technology 71(9) (2011) 1183-1189.
- [9] R. Mactabi, I.D. Rosca, S.V. Hoa, Monitoring the integrity of adhesive joints during fatigue loading using carbon nanotubes, Composites Science and Technology 78 (2013) 1-9.
- [10] W. Zhang, V. Sakalkar, N. Koratkar, In situ health monitoring and repair in composites using carbon nanotube additives, Applied Physics Letters 91(13) (2007).
- [11] M.H. Al-Saleh, U. Sundararaj, A review of vapor grown carbon nanofiber/polymer conductive composites, Carbon 47(1) (2009) 2-22.
- [12] R.B. Ladani, A.R. Ravindran, S. Wu, K. Pingkarawat, A.J. Kinloch, A.P. Mouritz, R.O. Ritchie, C.H. Wang, Multi-scale toughening of fibre composites using carbon nanofibres and z-pins, Composites Science and Technology 131 (2016) 98-109.
- [13] S. Wu, R.B. Ladani, J. Zhang, K. Ghorbani, X. Zhang, A.P. Mouritz, A.J. Kinloch, C.H. Wang, Strain Sensors with Adjustable Sensitivity by Tailoring the Microstructure of Graphene Aerogel/PDMS Nanocomposites, Acs Appl Mater Inter (2016).